JACS
JOURNAL OF THE AMERICAN CHEMICAL SOCIETY
pubs.acs.org/JACS
Communication

Polymorphism in the Ruddlesden–Popper Nickelate $La_3Ni_2O_7$: Discovery of a Hidden Phase with Distinctive Layer Stacking

Xinglong Chen,* Junjie Zhang, Arashdeep S. Thind, Shekhar Sharma, Harrison LaBollita, Gordon Peterson, Hong Zheng, Daniel P. Phelan, Antia S. Botana, Robert F. Klie, and J. F. Mitchell*

Cite This: J. Am. Chem. Soc. 2024, 146, 3640–3645

ABSTRACT: We report the discovery of a novel form of Ruddlesden–Popper (RP) nickelate that stands as the first example of long-range, coherent polymorphism in this class of inorganic solids. Rather than the well-known, uniform stacking of perovskite blocks ubiquitously found in RP phases, this newly discovered polymorph of the bilayer RP phase $La_3Ni_2O_7$ adopts a novel stacking sequence in which single-layer and trilayer blocks of NiO_6 octahedra alternate in a "1313" sequence. Crystals of this new polymorph are described in space group *Cmmm*, although we note evidence for a competing *Imam* variant. Transport measurements at ambient pressure reveal metallic character with evidence of a charge density wave transition with an onset at $T \approx 134$ K. The discovery of such polymorphism could reverberate to the expansive range of science and applications that rely on RP materials, particularly the recently reported signatures of superconductivity in bilayer $La_3Ni_2O_7$ with T_c as high as 80 K above 14 GPa.

The Ruddlesden–Popper (RP) oxides, $A_{n+1}B_nO_{3n+1}$ (A = alkaline earth or rare earth, B = transition metal; n = 1, 2, 3, ..., ∞), contain the structural motif of perovskite-like, n-layer slabs that are separated by double rocksalt layers. They are among the most well-studied inorganic solid state structure types.[1−9] Of particular importance is the notion that the dimensionality of their electronic structure evolves from quasi-two-dimensional to three-dimensional as n increases. This dimensionality effect, along with distortion and tilting of oxygen octahedra within the perovskite slabs, strongly affects the behavior of a wide variety of materials, including solid oxide fuel cells, photocatalysts, metal-air battery cathodes, and a plethora of quantum materials that exhibit magnetism, metal–insulator transitions, superconductivity, etc. For example, the RP nickelates $La_{n+1}Ni_nO_{3n+1}$ evolve from insulating, charge- and spin-stripe ordered states for n = 1,[10−15] to charge- and spin-density wave states for n = 2 and n = 3,[16−18] to a metallic, Pauli paramagnetic state for $n = \infty$.[19,20] Indeed, high temperature superconductivity has recently been reported for n = 2 and n = 3 compounds subjected to pressure, with n = 2 $La_3Ni_2O_7$ having a maximum reported $T_c \approx 80$ K (14 GPa)[21−25] and n = 3 $La_4Ni_3O_{10}$ $T_c \approx 25$ K (38 GPa).[26−28] These discoveries are intriguing since the octahedral coordination and electronic configuration of Ni (formally, $d^{7.5}$, $Ni^{2.5+}$ for $La_3Ni_2O_7$ and $d^{7.33}$, $Ni^{2.67+}$ for $La_4Ni_3O_{10}$) are far-removed from the strongly Jahn–Teller distorted, d^9, Cu^{2+} configuration of the superconducting cuprates.[29,30] These new results motivate the search for new RP nickelates that could support superconductivity or competing electronic states.

In this Letter, we report the discovery of polymorphic RP phases in bulk crystals of $La_3Ni_2O_7$ established by combining single-crystal X-ray diffraction (SC-XRD) and scanning transmission electron microscopy (STEM). The well-known n = 2 RP $La_3Ni_2O_7$ polymorph (hereafter referred to as LNO-2222) adopts a uniform "2222" stacking of bilayers (Figure 1a). In contrast, the newly discovered polymorph (LNO-1313 hereafter) assumes a novel stacking sequence in which single-layer and trilayer blocks of NiO_6 octahedra alternate in a "1313" sequence (Figure 1b). Transport measurements on an LNO-1313 crystal reveal its metallic character and the signature of a charge density wave (CDW) at $T \approx 134$ K. First-principles calculations indicate that the electronic structure of LNO-1313 can be described as a superposition of the individual single-layer and trilayer subsystems.

LNO-1313 single crystals were grown by a high oxygen pressure floating zone technique. During growth, competing phases include LNO-2222, trilayer $La_4Ni_3O_{10}$, and monolayer La_2NiO_4. Note that $La_4Ni_3O_{10}$ and La_2NiO_4 have been established as competing phases for LNO-2222 growth;[31] however, the "hidden" LNO-1313 had not been identified until we discovered it serendipitously due to its distinctive SC-XRD pattern. We reproduced the growth of LNO-1313 crystals across several crystal boules, but at this stage, the parameters that control the balance, selection, or distribution of phases during growth have not yet been fully identified. Since LNO-1313 has never been reported—despite the vast structural chemistry literature of polycrystalline bilayer RP phases—its appearance seems to be a consequence of growth from the melt.

Laboratory SC-XRD results reveal that LNO-1313 crystallizes in an orthorhombic space group with reflection conditions consistent with *Cmmm* (No. 65). Remarkably, as shown in

Received: December 12, 2023
Revised: January 22, 2024
Accepted: January 24, 2024
Published: January 31, 2024

https://doi.org/10.1021/jacs.3c14052
J. Am. Chem. Soc. 2024, 146, 3640–3645

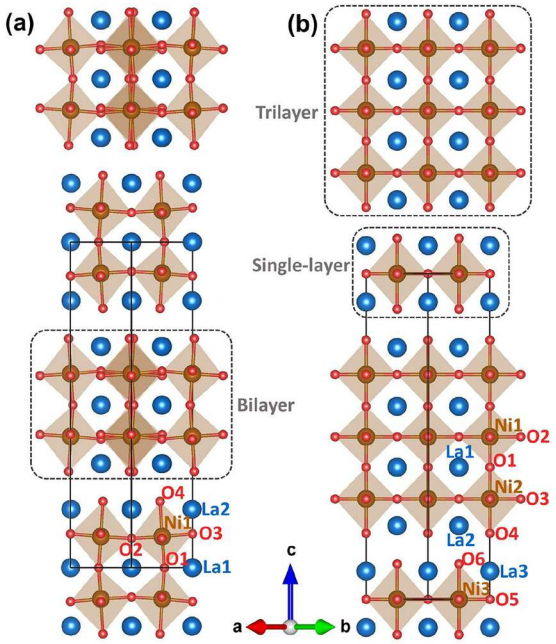

Figure 1. Polymorphic crystal structures of (a) LNO-2222 and (b) LNO-1313.

Figure 1b, rather than the expected uniform stacking of bilayers assembled from corner-shared NiO_6 octahedra, the LNO-1313 structure features an alternate stacking of single layers and trilayers. In other words, the LNO-1313 polymorph can be viewed as a periodic, 1:1 ordered intergrowth of La_2NiO_4 and $La_4Ni_3O_{10}$. While incoherent mixed stacking of layers has been reported in epitaxial films of RP phases,[32,33] to the best of our knowledge, no such bulk, long-range ordered polymorphic behavior has been reported in either oxide or nonoxide RP families.

The crystal data, structure refinement results, and bond lengths and bond angles of *Cmmm* LNO-1313 and *Amam* LNO-2222 are summarized in Table 1, with additional details in Tables S1−S9 in the Supporting Information (SI). While the unit cell volumes of these two phases are similar, the *a* and *b* axes of LNO-1313 are slightly longer than those of LNO-2222, while the *c* axis of LNO-1313 is slightly shorter. Rather than the buckled, ≈168° out-of-plane Ni1−O1−Ni1 angle found in LNO-2222, in *Cmmm* LNO-1313 the analogous angle (Ni1−O1−Ni2 in the trilayer block) is symmetry-constrained to 180°. Notably, this angle in trilayer RP $La_4Ni_3O_{10}$ *is* buckled.[30]

As shown in Figure 2, the experimental diffraction patterns of LNO-1313 and LNO-2222 are quite distinct, especially along c^*. We describe both cells consistently (Table 1) with $a < b < c$. Consider first the $(hk0)$ plane. Although LNO-1313 and LNO-2222 share the feature that prominent reflections are all observed at $h = 2n$, $k = 2n$, a set of weaker reflections (marked by open circles) can be used to distinguish their different centering modes, *C* and *A*, respectively. Additionally, in the $(0kl)$ plane, the reflection density along c^* in LNO-1313 is twice that found for LNO-2222, clearly distinguishing the two polymorphs. For LNO-2222, the distinct reflections at $k = 2n + 1$, $l = 2n + 1$ unambiguously demonstrate its *A* centering $(k + l = 2n)$ rather than *F* centering ($k = 2n$, $l = 2n$ in $(0kl)$), which has been proposed for LNO-2222 by some authors.[34] A more thorough analysis is provided in the SI.

We measured more than ten LNO-1313 specimens, all of which can be satisfactorily solved using the *Cmmm* model. However, in some specimens, weak half-integer reflections were observed in the $(0kl)$ plane (see Figure S1). These

Table 1. Crystal Data, Structure Refinement, and Selected Bond Lengths and Angles for $La_3Ni_2O_7$ Polymorphs[a]

Identification code	LNO-1313	LNO-2222
Formula	$La_3Ni_2O_7$	$La_3Ni_2O_7$
Space group	*Cmmm* (No. 65)	*Amam* (No. 63)
a/Å	5.4382(5)	5.4053(6)
b/Å	5.4700(5)	5.4536(6)
c/Å	20.3598(19)	20.517(2)
Volume/Å^3	605.64(10)	604.80(12)
Index ranges/h,k,l	[−6, 6], [−6, 6], [−25, 25]	[−7, 7], [−7, 7], [−29, 29]
Final *R* indices $[I \geq 2\sigma(I)]$	$R_1 = 0.0238$, $wR_2 = 0.0458$	$R_1 = 0.0202$, $wR_2 = 0.0527$
Largest diff. peak/hole/e Å^{-3}	0.99/−1.70	1.31/−1.14
In-plane Ni−O/Å	Ni1−O2: 1.92832(12) Ni2−O3: 1.92833(13) Ni3−O5: 1.92832(13)	Ni1−O2: 1.9335(5) Ni1−O3: 1.9183(6)
Out-of-plane Ni−O/Å	Ni1−O1: 1.902(13) Ni2−O1: 1.986(13) Ni2−O4: 2.150(13) Ni3−O6: 2.211(12)	Ni1−O1: 1.9816(11) Ni1−O4: 2.231(4)
In-plane Ni−O−Ni/deg	Ni1−O2−Ni1: 180 Ni2−O3−Ni2: 179.7(5) Ni3−O5−Ni3: 180	Ni1−O2−Ni1: 172.0(2) Ni1−O3−Ni1: 169.6(3)
Out-of-plane Ni−O−Ni/deg	Ni1−O1−Ni2: 180	Ni1−O1−Ni1: 168.1(3)

[a]Note: Values in parentheses are the estimated standard deviation from the refinement.

https://doi.org/10.1021/jacs.3c14052
J. Am. Chem. Soc. 2024, 146, 3640−3645

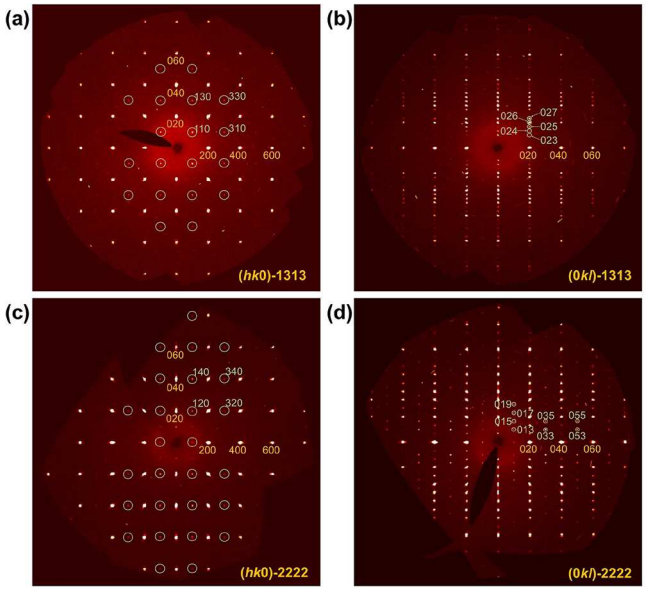

Figure 2. Precession images of LNO-1313 and LNO-2222 crystals. (a) (*hk*0) for LNO-1313; (b) (0*kl*) for LNO-1313; (c) (*hk*0) for LNO-2222; (d) (0*kl*) for LNO-2222.

reflections indicate the possibility of *c*-axis doubling and symmetry lowering consistent with *Imam* (alternate setting of *Imma*, No. 74). Importantly, this symmetry lowering preserves the "1313" stacking in the structure. Unfortunately, SC-XRD data alone preclude us from distinguishing whether these specimens are purely *Imam* or a mixture of *Cmmm* and *Imam* regions in the specimen. Further details, including evidence for little to no non-stoichiometry of O, are provided in the SI.

STEM was employed to investigate the real-space atomic structure and stacking sequence of LNO-1313 and LNO-2222 single crystals. As shown in Figure 3a and 3b, atomic-

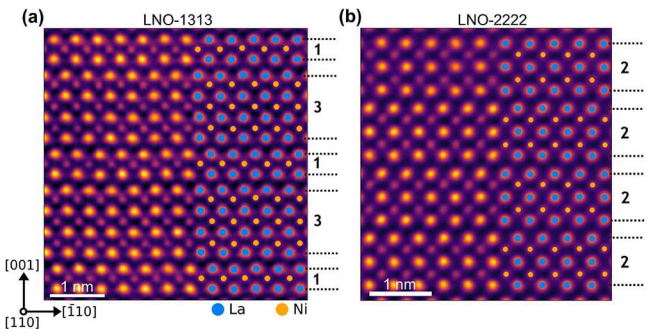

Figure 3. Atomic resolution STEM-HAADF images along the [110] orientation with La and Ni atoms labeled (a) LNO-1313 and (b) LNO-2222.

resolution high-angle annular dark-field (HAADF) images along the [110] crystallographic orientation clearly reveal distinguishable La (Z = 57) and Ni (Z = 28) atomic columns. Based on the cation sublattice, the "1313" and "2222" stacking sequences can be resolved for the respective polymorphs, and the measured atomic distances agree well with the SC-XRD models for *Cmmm* LNO-1313 and *Amam* LNO-2222. In addition, the LNO-1313 specimen was observed to have a very low density of stacking faults. Details of chemical composition, stacking faults, atomic distance analysis, and HAADF image along [100] can be found in the SI.

Figure 4 shows the normalized *ab*-plane resistivity of LNO-1313, LNO-2222, and $La_4Ni_3O_{10}$ single crystals between 1.8

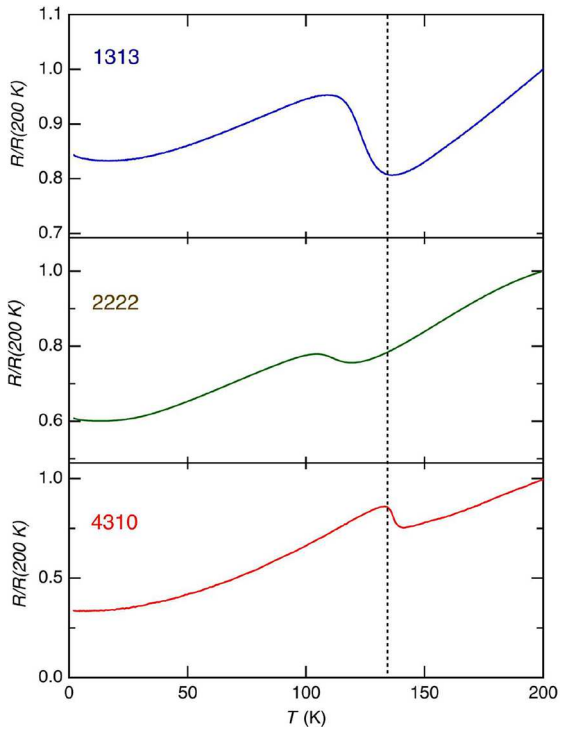

Figure 4. Electrical resistivity of LNO-1313, LNO-2222, and $La_4Ni_3O_{10}$ single crystals. The vertical dashed line marks the LNO-1313 transition onset determined by a tangent construction.

and 200 K, all of which generally decrease with decreasing temperature, characteristic of a metal. For LNO-1313, a pronounced anomaly associated with a metal-to-metal transition (MMT) is observed with an onset of $T_{MMT} \approx 134$ K. This electrical transport behavior resembles that of $La_4Ni_3O_{10}$ ($T_{MMT} \approx 139$ K) and the LNO-2222 polymorph of $La_3Ni_2O_7$ ($T_{MMT} \approx 122$ K). In these cases, the anomaly has been either shown to be a CDW by X-ray diffraction ($La_4Ni_3O_{10}$)[17] or speculated to be such ($La_3Ni_2O_7$).[16]

We studied the nonmagnetic electronic structure of the *Cmmm* using first-principles calculations. The band structure with the band character plot of LNO-1313 (with $d^{7.5}$ filling) is shown in Figure 5. The most remarkable finding is that the

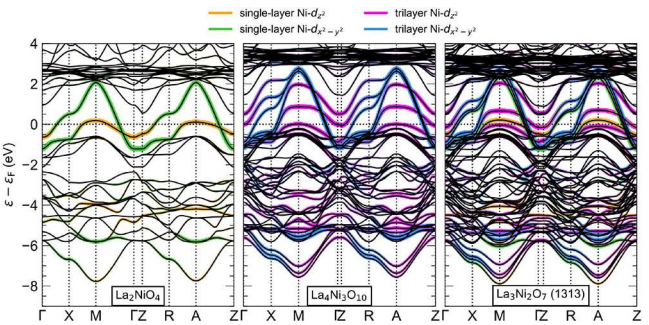

Figure 5. Electronic structures of LNO-1313 (*Cmmm*), La_2NiO_4, and $La_4Ni_3O_{10}$. The orbital-resolved band structure along high-symmetry lines is shown, highlighting the Ni-d_{z^2} (orange for the single-layer Ni, pink for trilayer Ni atoms) and Ni-$d_{x^2-y^2}$ (green for the single-layer Ni, blue for the trilayer Ni atoms) orbital weights.[36]

https://doi.org/10.1021/jacs.3c14052
J. Am. Chem. Soc. 2024, 146, 3640−3645

band structure seems to be an electronic superposition of the single-layer (La_2NiO_4) and trilayer ($La_4Ni_3O_{10}$) subsystems at low-energy (although the superposition is not exact because of charge transfer from the formally $Ni^{8/3+}$ trilayer to the Ni^{2+} single-layer to satisfy the $d^{7.5}$ electron count). This superposition is particularly noticeable when considering the dominant e_g states around the Fermi level, where four Ni-$d_{x^2-y^2}$ and four Ni-d_{z^2} bands can be seen (one from the single-layer Ni atoms and three from the trilayer Ni atoms). For the d_{z^2} states, the bonding, nonbonding, and antibonding bands from the Ni-d_{z^2} triplet of the trilayer can be clearly appreciated.[35] This contrasts with the usual bonding−antibonding complex found in the LNO-2222 bilayer polymorph (Fermi surfaces and a comparison between the LNO-2222 and LNO-1313 electronic structures are shown in the SI). The fact that the electronic structure of $La_4Ni_3O_{10}$ underlies that of LNO-1313 is consistent with the similarities in the resistivity described above.

The report of superconductivity signatures in $La_3Ni_2O_7$ with T_c up to 80 K under pressure represents a potential breakthrough in the quest for bulk nickelate superconductivity.[21] As mentioned earlier, both bilayer LNO-2222 and trilayer $La_4Ni_3O_{10}$ show CDW order in electrical transport measurements.[16,17] Under pressure, this CDW order is suppressed toward T = 0, interrupted by the emergence of the superconducting transition. Structural studies have found that the buckled Ni−O−Ni linkage joining octahedral layers in the bilayer straightens with application of pressure, coincident with the onset of superconductivity.[21,37] Indeed, several authors argue that this structural response may be a prerequisite for superconductivity.[38,39] However, the proposed *Cmmm* structure of ambient-pressure, nonsuperconducting LNO-1313 already contains 180° Ni−O−Ni linkages in the trilayer block, implying that this structural feature alone may be insufficient to stabilize the superconducting state. We note that in the putative *Imam* structure, which we have not been able to satisfactorily refine from SC-XRD data (see SI), buckling is possible and might respond to pressure.

Curiously, in bilayer nickelates a true zero-resistance state is not universally found, and in certain samples, *no* superconducting transition is found.[40] Speculation that this inconsistency could signal filamentary superconductivity arising from a second unidentified phase in the bulk $La_3Ni_2O_7$ crystal has been strengthened by recent magnetic susceptibility measurements that reveal a rather low (approximately 1%) superconducting volume fraction in $La_3Ni_2O_7$ crystals under pressure.[41] While highly speculative, it is possible that one or more phases competing with LNO-2222 in the crystal growth, such as LNO-1313 (*Cmmm* and/or *Imam*), could be a source of superconductivity. Measurements of LNO-1313 transport under pressure are essential to test this possibility and are underway.

In conclusion, we report a new form of alternating n = 1 and n = 3 perovskite slab layers in an ordered RP oxide phase, $La_3Ni_2O_7$. Two polymorphic stacking sequences—the known LNO-2222 and the new LNO-1313—are found during crystal growth at high pO_2. The discovery of these two polymorphs could fundamentally impact the rapidly evolving field of RP nickelate superconductivity. More broadly, the mere existence of such polymorphism suggests that similar polymorphism may be found in RP phases other than $La_3Ni_2O_7$ under suitable synthesis conditions. Such new compounds could harbor novel properties, with potential impact for the wide range of fundamental and applied science that rely on members of this expansive layered perovskite family.

Author's Note: During review of this manuscript, we became aware of several preprints on the mixed layered RP nickelates that appeared subsequent to our submission: P. Puphal et al. reported the discovery of "1313" stacking in $La_3Ni_2O_7$ and conducted a high pressure study on both as-grown and annealed $La_3Ni_2O_7$ crystals;[42] F. Li et al. reported another novel mixed layered nickelates with "1212" stacking grown by a flux method at ambient pressure;[43] H. Wang et al. reported the floating zone growth and structural study of both polymorphs of $La_3Ni_2O_7$ and found *Cmmm* symmetry for LNO-1313.[44]

■ ASSOCIATED CONTENT

Supporting Information

The Supporting Information is available free of charge at https://pubs.acs.org/doi/10.1021/jacs.3c14052.

Methods for crystal growth, SC-XRD structure determination, Electron Microscopy, computational studies, and electrical resistivity; additional results and discussion on crystal structure, electron microscopy, and theoretical calculations; tables of crystallographic data (PDF)

Accession Codes

CCDC 2313278 and 2313280 contain the supplementary crystallographic data for this paper. These data can be obtained free of charge via www.ccdc.cam.ac.uk/data_request/cif, or by emailing data_request@ccdc.cam.ac.uk, or by contacting The Cambridge Crystallographic Data Centre, 12 Union Road, Cambridge CB2 1EZ, UK; fax: +44 1223 336033.

■ AUTHOR INFORMATION

Corresponding Authors

Xinglong Chen − *Materials Science Division, Argonne National Laboratory, Lemont, Illinois 60439, United States;* orcid.org/0000-0003-2283-7293; Email: xinglong.chen@anl.gov

J. F. Mitchell − *Materials Science Division, Argonne National Laboratory, Lemont, Illinois 60439, United States;* orcid.org/0000-0002-8416-6424; Email: mitchell@anl.gov

Authors

Junjie Zhang − *Materials Science Division, Argonne National Laboratory, Lemont, Illinois 60439, United States;* Present Address: Current Affiliation: Institute of Crystal Materials, Shandong University, Shandong, China; orcid.org/0000-0002-5561-1330

Arashdeep S. Thind − *Department of Physics, University of Illinois—Chicago, Chicago, Illinois 60607, United States*

Shekhar Sharma − *Department of Physics and Astronomy, Arizona State University, Tempe, Arizona 85218, United States*

Harrison LaBollita − *Department of Physics and Astronomy, Arizona State University, Tempe, Arizona 85218, United States*

Gordon Peterson − *Materials Science Division, Argonne National Laboratory, Lemont, Illinois 60439, United States*

Hong Zheng − *Materials Science Division, Argonne National Laboratory, Lemont, Illinois 60439, United States*

Daniel P. Phelan − *Materials Science Division, Argonne National Laboratory, Lemont, Illinois 60439, United States*

Antia S. Botana − *Department of Physics and Astronomy, Arizona State University, Tempe, Arizona 85218, United States*

Robert F. Klie − *Department of Physics, University of Illinois—Chicago, Chicago, Illinois 60607, United States;* orcid.org/0000-0003-4773-6667

Complete contact information is available at: https://pubs.acs.org/10.1021/jacs.3c14052

Notes

The authors declare no competing financial interest.

■ ACKNOWLEDGMENTS

Work at Argonne National Laboratory (crystal growth, structural determinations, transport measurements) was sponsored by the US Department of Energy, Office of Science, Basic Energy Sciences, Materials Science and Engineering Division. Work at UIC (microscopy) was supported by a grant from the National Science Foundation (NSF-DMR 22). Acquisition of the UIC JEOL ARM200CF was supported by an MRI-R2 grant from the National Science Foundation (DMR-0959470). The Gatan Continuum GIF acquisition at UIC was supported by an MRI grant from the National Science Foundation (DMR-1626065). This work made use of the ThermoFisher Helios 5CX (cryo) FIB-SEM instrument in the Electron Microscopy Core of UIC's Research Resources Center, which received support from UIC, Northwestern University and ARO (W911NF2110052). Work at ASU (theoretical calculations) was supported by NSF grant no. DMR-2045826 and the ASU Research Computing Center.

■ REFERENCES

(1) Ruddlesden, S. N.; Popper, P. New Compounds of the K_2NiF_4 Type. *Acta Crystallogr.* **1957**, *10* (8), 538−539.

(2) Ding, P.; Li, W.; Zhao, H.; Wu, C.; Zhao, L.; Dong, B.; Wang, S. Review on Ruddlesden-Popper Perovskites as Cathode for Solid Oxide Fuel Cells. *J. Phys. Mater.* **2021**, *4* (2), No. 022002.

(3) Yoshida, S.; Akamatsu, H.; Tsuji, R.; Hernandez, O.; Padmanabhan, H.; Sen Gupta, A.; Gibbs, A. S.; Mibu, K.; Murai, S.; Rondinelli, J. M.; Gopalan, V.; Tanaka, K.; Fujita, K. Hybrid Improper Ferroelectricity in $(Sr,Ca)_3Sn_2O_7$ and Beyond: Universal Relationship between Ferroelectric Transition Temperature and Tolerance Factor in n = 2 Ruddlesden-Popper Phases. *J. Am. Chem. Soc.* **2018**, *140* (46), 15690−15700.

(4) Uppuluri, R.; Akamatsu, H.; Sen Gupta, A.; Wang, H.; Brown, C. M.; Agueda Lopez, K. E.; Alem, N.; Gopalan, V.; Mallouk, T. E. Competing Polar and Antipolar Structures in the Ruddlesden-Popper Layered Perovskite $Li_2SrNb_2O_7$. *Chem. Mater.* **2019**, *31* (12), 4418−4425.

(5) Takeguchi, T.; Yamanaka, T.; Takahashi, H.; Watanabe, H.; Kuroki, T.; Nakanishi, H.; Orikasa, Y.; Uchimoto, Y.; Takano, H.; Ohguri, N.; Matsuda, M.; Murota, T.; Uosaki, K.; Ueda, W. Layered Perovskite Oxide: A Reversible Air Electrode for Oxygen Evolution/Reduction in Rechargeable Metal-Air Batteries. *J. Am. Chem. Soc.* **2013**, *135* (30), 11125−11130.

(6) Mulder, A. T.; Benedek, N. A.; Rondinelli, J. M.; Fennie, C. J. Turning ABO_3 Antiferroelectrics into Ferroelectrics: Design Rules for Practical Rotation-Driven Ferroelectricity in Double Perovskites and $A_3B_2O_7$ Ruddlesden-Popper Compounds. *Adv. Funct. Mater.* **2013**, *23* (38), 4810−4820.

(7) Zhang, R.; Senn, M. S.; Hayward, M. A. Directed Lifting of Inversion Symmetry in Ruddlesden-Popper Oxide-Fluorides: Toward Ferroelectric and Multiferroic Behavior. *Chem. Mater.* **2016**, *28* (22), 8399−8406.

(8) Forslund, R. P.; Hardin, W. G.; Rong, X.; Abakumov, A. M.; Filimonov, D.; Alexander, C. T.; Mefford, J. T.; Iyer, H.; Kolpak, A. M.; Johnston, K. P.; Stevenson, K. J. Exceptional Electrocatalytic Oxygen Evolution via Tunable Charge Transfer Interactions in $La_{0.5}Sr_{1.5}Ni_{1-x}Fe_xO_{4\pm\delta}$ Ruddlesden-Popper Oxides. *Nat. Commun.* **2018**, *9* (1), 3150.

(9) Sivakumar, T.; Seshadri, R.; Gopalakrishnan, J. Bridging the Ruddlesden-Popper and the Aurivillius Phases: Synthesis and Structure of a Novel Series of Layered Perovskite Oxides, (BiO)-$LnTiO_4$ (Ln = La, Nd, Sm). *J. Am. Chem. Soc.* **2001**, *123* (46), 11496−11497.

(10) Chen, C. H.; Cheong, S. W.; Cooper, A. S. Charge modulations in $La_{2-x}Sr_xNiO_{4+y}$: Ordering of Polarons. *Phys. Rev. Lett.* **1993**, *71* (15), 2461−2464.

(11) Ramirez, A. P.; Gammel, P. L.; Cheong, S. W.; Bishop, D. J.; Chandra, P. Charge Modulation in $La_{1.67}Sr_{0.33}NiO_4$: A Bulk Thermodynamic Study. *Phys. Rev. Lett.* **1996**, *76* (3), 447−450.

(12) Abeykoon, A. M. M.; Božin, E. S.; Yin, W.-G.; Gu, G.; Hill, J. P.; Tranquada, J. M.; Billinge, S. J. L. Evidence for Short-Range-Ordered Charge Stripes Far above the Charge-Ordering Transition in $La_{1.67}Sr_{0.33}NiO_4$. *Phys. Rev. Lett.* **2013**, *111* (9), No. 096404.

(13) Anissimova, S.; Parshall, D.; Gu, G. D.; Marty, K.; Lumsden, M. D.; Chi, S.; Fernandez-Baca, J. A.; Abernathy, D. L.; Lamago, D.; Tranquada, J. M.; Reznik, D. Direct Observation of Dynamic Charge Stripes in $La_{2-x}Sr_xNiO_4$. *Nat. Commun.* **2014**, *5* (1), 3467.

(14) Lee, S. H.; Cheong, S. W. Melting of Quasi-Two-Dimensional Charge Stripes in $La_{5/3}Sr_{1/3}NiO_4$. *Phys. Rev. Lett.* **1997**, *79* (13), 2514−2517.

(15) Lee, S. H.; Tranquada, J. M.; Yamada, K.; Buttrey, D. J.; Li, Q.; Cheong, S. W. Freezing of a Stripe Liquid. *Phys. Rev. Lett.* **2002**, *88* (12), No. 126401.

(16) Liu, Z.; Sun, H.; Huo, M.; Ma, X.; Ji, Y.; Yi, E.; Li, L.; Liu, H.; Yu, J.; Zhang, Z.; Chen, Z.; Liang, F.; Dong, H.; Guo, H.; Zhong, D.; Shen, B.; Li, S.; Wang, M. Evidence for Charge and Spin Density Waves in Single Crystals of $La_3Ni_2O_7$ and $La_3Ni_2O_6$. *Sci. Chin. Phys. Mech. Astron.* **2023**, *66* (1), No. 217411.

(17) Zhang, J.; Phelan, D.; Botana, A. S.; Chen, Y. S.; Zheng, H.; Krogstad, M.; Wang, S. G.; Qiu, Y.; Rodriguez-Rivera, J. A.; Osborn, R.; Rosenkranz, S.; Norman, M. R.; Mitchell, J. F. Intertwined Density Waves in a Metallic Nickelate. *Nat. Commun.* **2020**, *11* (1), 6003.

(18) Chen, X.; Jiang, P.; Li, J.; Zhong, Z.; Lu, Y. Critical Charge and Spin Instabilities in Superconducting $La_3Ni_2O_7$. **2023**, arXiv:2307.07154. arXiv. DOI: 10.48550/arXiv.2307.07154. (accessed January 22, 2024).

(19) Sreedhar, K.; Honig, J. M.; Darwin, M.; McElfresh, M.; Shand, P. M.; Xu, J.; Crooker, B. C.; Spalek, J. Electronic Properties of the Metallic Perovskite $LaNiO_3$: Correlated Behavior of 3d Electrons. *Phys. Rev. B* **1992**, *46* (10), 6382−6386.

(20) Zhou, J. S.; Goodenough, J. B.; Dabrowski, B. Transition from Curie-Weiss to Enhanced Pauli Paramagnetism in $RNiO_3$ (R=La,Pr,⋯ Gd). *Phys. Rev. B* **2003**, *67* (2), No. 020404.

(21) Sun, H.; Huo, M.; Hu, X.; Li, J.; Liu, Z.; Han, Y.; Tang, L.; Mao, Z.; Yang, P.; Wang, B.; Cheng, J.; Yao, D. X.; Zhang, G. M.; Wang, M. Signatures of Superconductivity Near 80 K in a Nickelate under High Pressure. *Nature* **2023**, *621* (7979), 493−498.

(22) Hou, J.; Yang, P.-T.; Liu, Z.-Y.; Li, J.-Y.; Shan, P.-F.; Ma, L.; Wang, G.; Wang, N.-N.; Guo, H.-Z.; Sun, J.-P.; Uwatoko, Y.; Wang, M.; Zhang, G.-M.; Wang, B.-S.; Cheng, J.-G. Emergence of High-Temperature Superconducting Phase in Pressurized $La_3Ni_2O_7$ Crystals. *Chin. Phys. Lett.* **2023**, *40* (11), No. 117302.

(23) Zhang, Y.; Su, D.; Huang, Y.; Sun, H.; Huo, M.; Shan, Z.; Ye, K.; Yang, Z.; Li, R.; Smidman, M.; Wang, M.; Jiao, L.; Yuan, H. High-Temperature Superconductivity with Zero-Resistance and Strange Metal Behavior in $La_3Ni_2O_7$. **2023**, arXiv:2307.14819. arXiv. DOI: 10.48550/arXiv.2307.14819 (accessed January 22, 2024).

(24) Wang, G.; Wang, N.; Hou, J.; Ma, L.; Shi, L.; Ren, Z.; Gu, Y.; Shen, X.; Ma, H.; Yang, P.; Liu, Z.; Guo, H.; Sun, J.; Zhang, G.; Yan, J.; Wang, B.; Uwatoko, Y.; Cheng, J. Pressure-Induced Super-

conductivity in Polycrystalline $La_3Ni_2O_7$. **2023**, arXiv:2309.17378. arXiv. DOI: 10.48550/arXiv.2309.17378 (accessed January 22, 2024).
(25) Zhang, M.; Pei, C.; Wang, Q.; Zhao, Y.; Li, C.; Cao, W.; Zhu, S.; Wu, J.; Qi, Y. Effects of Pressure and Doping on Ruddlesden-Popper Phases $La_{n+1}Ni_nO_{3n+1}$. *J. Mater. Sci. Technol.* **2024**, *185*, 147−154.
(26) Zhang, M.; Pei, C.; Du, X.; Cao, Y.; Wang, Q.; Wu, J.; Li, Y.; Zhao, Y.; Li, C.; Cao, W.; Zhu, S.; Zhang, Q.; Yu, N.; Cheng, P.; Zhao, J.; Chen, Y.; Guo, H.; Yang, L.; Qi, Y. Superconductivity in Trilayer Nickelate $La_4Ni_3O_{10}$ under Pressure. **2023**, arXiv:2311.07423. arXiv. DOI: 10.48550/arXiv.2311.07423 (accessed January 22, 2024).
(27) Zhu, Y.; Zhang, E.; Pan, B.; Chen, X.; Chen, L.; Ren, H.; Liu, F.; Wang, J.; Jia, D.; Wo, H.; Gu, Y.; Gu, Y.; Ji, L.; Wang, W.; Gou, H.; Shen, Y.; Ying, T.; Guo, J.; Zhao, J. Superconductivity in Trilayer $La_4Ni_3O_{10}$ Single Crystals. **2023**, arXiv:2311.07353. arXiv. DOI: 10.48550/arXiv.2311.07353 (accessed January 22, 2024).
(28) Li, Q.; Zhang, Y.-J.; Xiang, Z.-N.; Zhang, Y.; Zhu, X.; Wen, H.-H. Signature of superconductivity in pressurized $La_4Ni_3O_{10}$. *Chin. Phys. Lett.* **2024**, *41*, No. 017401.
(29) Bednorz, J. G.; Müller, K. A. Possible High T_c Superconductivity in the Ba−La−Cu−O System. *Z. Phys. B Condens. Matter.* **1986**, *64* (2), 189−193.
(30) Keimer, B.; Kivelson, S. A.; Norman, M. R.; Uchida, S.; Zaanen, J. From Quantum Matter to High-Temperature Superconductivity in Copper Oxides. *Nature* **2015**, *518* (7538), 179−186.
(31) Zhang, J.; Zheng, H.; Chen, Y.-S.; Ren, Y.; Yonemura, M.; Huq, A.; Mitchell, J. F. High Oxygen Pressure Floating Zone Growth and Crystal Structure of the Metallic Nickelates $R_4Ni_3O_{10}$ (R = La, Pr). *Phys. Rev. Mater.* **2020**, *4*, No. 083402.
(32) Burriel, M.; Garcia, G.; Rossell, M. D.; Figueras, A.; Van Tendeloo, G.; Santiso, J. Enhanced High-Temperature Electronic Transport Properties in Nanostructured Epitaxial Thin Films of the $La_{n+1}Ni_nO_{3n+1}$ Ruddlesden-Popper Series (n = 1, 2, 3, ∞). *Chem. Mater.* **2007**, *19* (16), 4056−4062.
(33) Ram, R. A. M.; Ganapathi, L.; Ganguly, P.; Rao, C. N. R. Evolution of Three-dimensional Character Across the $La_{n+1}Ni_nO_{3n+1}$ Homologous Series with Increase in *n*. *J. Solid State Chem.* **1986**, *63* (2), 139−147.
(34) Park, J.-C.; Kim, D.-K.; Byeon, S.-H.; Kim, D. XANES Study on Ruddlesden-Popper Phase, $La_{n+1}Ni_nO_{3n+1}$ (n = 1, 2, and ∞). *J. Synchrotron Radiat.* **2001**, *8* (2), 704−706.
(35) Jung, M.-C.; Kapeghian, J.; Hanson, C.; Pamuk, B.; Botana, A. S. Electronic Structure of Higher-Order Ruddlesden-Popper Nickelates. *Phys. Rev. B* **2022**, *105* (8), No. 085150.
(36) We use tetragonal structures for the single-layer and trilayer nickelates to make the comparison of the electronic structures easier to follow. We showed in previous work that this does not affect the description of the electronic structure when compared to experiments (see ref 35).
(37) Wang, L.; Li, Y.; Xie, S.; Liu, F.; Sun, H.; Huang, C.; Gao, Y.; Nakagawa, T.; Fu, B.; Dong, B.; Cao, Z.; Yu, R.; Kawaguchi, S. I.; Kadobayashi, H.; Wang, M.; Jin, C.; Mao, H.-k.; Liu, H. Structure Responsible for the Superconducting State in $La_3Ni_2O_7$ at High Pressure and Low Temperature Conditions. **2023**, arXiv:2311.09186. arXiv. DOI: 10.48550/arXiv.2311.09186 (accessed January 22, 2024).
(38) Geisler, B.; Hamlin, J. J.; Stewart, G. R.; Hennig, R. G.; Hirschfeld, P. J. Structural Transitions, Octahedral Rotations, and Electronic Properties of $A_3Ni_2O_7$ Rare-Earth Nickelates under High Pressure. **2023**, arXiv:2309.15078. arXiv. DOI: 10.48550/arXiv.2309.15078 (accessed January 22, 2024).
(39) Sakakibara, H.; Ochi, M.; Nagata, H.; Ueki, Y.; Sakurai, H.; Matsumoto, R.; Terashima, K.; Hirose, K.; Ohta, H.; Kato, M.; Takano, Y.; Kuroki, K. Theoretical Analysis on the Possibility of Superconductivity in a Trilayer Ruddlesden-Popper Nickelate $La_4Ni_3O_{10}$ under Pressure and Its Experimental Examination: Comparison with $La_3Ni_2O_7$. **2023**, arXiv:2309.09462. arXiv. DOI: 10.48550/arXiv.2309.09462 (accessed January 22, 2024).
(40) Gao, R.; Jin, L.; Huyan, S.; Ni, D.; Wang, H.; Xu, X.; Budko, S. L.; Canfield, P.; Xie, W.; Cava, R. J. Is $La_3Ni_2O_{6.5}$ a Bulk Superconducting Nickelate? **2023**, arXiv:2311.11122. arXiv. DOI: 10.48550/arXiv.2311.11122 (accessed January 22, 2024).
(41) Zhou, Y.; Guo, J.; Cai, S.; Sun, H.; Wang, P.; Zhao, J.; Han, J.; Chen, X.; Wu, Q.; Ding, Y.; Wang, M.; Xiang, T.; Mao, H.-K.; Sun, L. Evidence of Filamentary Superconductivity in Pressurized $La_3Ni_2O_7$ Single Crystals. **2023**, arXiv:2311.12361. arXiv. DOI: 10.48550/arXiv.2311.12361 (accessed January 22, 2024).
(42) Puphal, P.; Reiss, P.; Enderlein, N.; Wu, Y.-M.; Khaliullin, G.; Sundaramurthy, V.; Priessnitz, T.; Knauft, M.; Richter, L.; Isobe, M.; van Aken, P. A.; Takagi, H.; Keimer, B.; Suyolcu, Y. E.; Wehinger, B.; Hansmann, P.; Hepting, M. Unconventional Crystal Structure of the High-Pressure Superconductor $La_3Ni_2O_7$. **2023**, arXiv:2312.07341. arXiv. DOI: 10.48550/arXiv.2312.07341 (accessed January 22, 2024).
(43) Li, F.; Guo, N.; Zheng, Q.; Shen, Y.; Wang, S.; Cui, Q.; Liu, C.; Wang, S.; Tao, X.; Zhang, G.-M.; Zhang, J. Design and Synthesis of Three-Dimensional Hybrid Ruddlesden-Popper Nickelate Single Crystals. **2023**, arXiv:2312.08116. arXiv. DOI: 10.48550/arXiv.2312.08116 (accessed January 22, 2024).
(44) Wang, H.; Chen, L.; Rutherford, A.; Zhou, H.; Xie, W. Long-Range Structural Order in a Hidden Phase of Ruddlesden-Popper Bilayer Nickelates $La_3Ni_2O_7$. **2023**, arXiv:2312.09200. arXiv. DOI: 10.48550/arXiv.2312.09200 (accessed January 22, 2024).